Peer Community Journal

Section: Paleontology

RESEARCH ARTICLE

Published
2021-11-26

Cite as
Baptiste Suchéras-Marx, Fabienne Giraud, Alexandre Simionovici, Rémi Tucoulou and Isabelle Daniel (2021) *Evidence of high Sr/Ca in a Middle Jurassic murolith coccolith species*, Peer Community Journal, 1: e25.

Correspondence
sucheras-marx@cerege.fr

Peer-review
Peer reviewed and recommended by PCI Paleontology, https://doi.org/10.24072/pci.paleo.100006

Evidence of high Sr/Ca in a Middle Jurassic murolith coccolith species

Baptiste Suchéras-Marx [1], Fabienne Giraud [2,3], Alexandre Simionovici [2,4,3], Rémi Tucoulou [5], and Isabelle Daniel [6]

Volume **1** (2021), article e25

https://doi.org/10.24072/pcjournal.20

Abstract

Paleoceanographical reconstructions are often based on microfossil geochemical analyses. Coccoliths are the most ancient, abundant and continuous record of pelagic photic zone calcite producer organisms. Hence, they could be valuable substrates for geochemically based paleoenvironmental reconstructions but only Sr/Ca is exploited even if it remains poorly understood. For example, some murolith coccoliths species have very high Sr/Ca compared to the common 1-4 mmol/mol recorded in placolith coccoliths. In this study, we analyzed the elemental composition of the Middle Jurassic murolith *Crepidolithus crassus* by synchrotron-based nanoXRF (X-ray Fluorescence Spectroscopy) mapping focusing on Sr/Ca and compared the record to two placolith species, namely *Watznaueria contracta* and *Discorhabdus striatus*. In*C. crassus*, Sr/Ca is more than ten times higher than in both placoliths and seems higher in the proximal cycle. By comparison with the placoliths analyzed in the same analytical set-up and from the same sample, we exclude the impact of the diagenesis and seawater Sr/Ca to explain the high Sr/Ca in *C. crassus*. Based on comparisons to *Pontosphaera discopora* and *Scyphosphaera apsteinii* which also have high Sr/Ca, it seems more likely that high Sr/Ca in *C. crassus* is either due to the vertical elongation of the R-units of the proximal cycle or related to the action of the special polysaccharide controlling the growth of those vertically elongated R-units that may have affinities to Sr2+. In order to apply the Sr/Ca proxy to muroliths, further investigations are needed on cultured coccoliths.

[1]Aix Marseille Univ, CNRS, IRD, INRAE, Coll France, CEREGE - Aix-en-Provence, France, [2]CNRS, ISTerre – Grenoble, France, [3]Université Grenoble-Alpes, ISTerre – Grenoble, France, [4]Institut Universitaire de France (IUF), [5]ESRF – The European Synchrotron Radiation Facility – Grenoble, France, [6]UMR CNRS 5276 LGL, Université Claude Bernard Lyon 1, Ecole Normale Supérieure de Lyon – Villeurbanne, France

1. Introduction

Paleoceanography partly relies on the application of geochemical proxies – *i.e.* chemical changes of fossils or sediments composition induced by chemical, physical or biological parameters changing through time. Many geochemical proxies are based on elemental ratios in planktic or benthic foraminifera *e.g.* Mg/Ca (temperature; Elderfield & Ganssen, 2000), B/Ca (pH, Yu et al., 2007), U/Ca (carbonate saturation, Raitzsch et al., 2011), Cd/Ca (paleonutrient, Rickaby & Elderfield, 1999). Conversely, calcareous nannofossils – the micrometric platelets called coccoliths produced by the photosynthetic unicellular algae called coccolithophore and other micrometric calcite *incertae sedis* – are rarely used for geochemistry in paleoceanography. The rarity of nannofossil-based geochemical paleoproxies is linked to the very small size of calcareous nannofossils – *i.e.* ~1-15 µm – increasing the difficulty to isolate them from the rest of the sediment (Stoll & Ziveri, 2002; Stoll & Shimizu, 2009; Minoletti et al., 2009; Suchéras-Marx et al., 2016a). The only proxy commonly based on the calcareous nannofossil chemical composition is the Sr/Ca ratio used as a paleoproductivity proxy (Stoll & Schrag, 2000).

The most important factors influencing Sr/Ca ratios in biogenic carbonates is outlined in Ullmann et al. (2013) and are i) the composition of the liquid from which they are precipitated (modern oceans ~8 mmol/mol (Lebrato et al., 2020); Middle Jurassic ~5 mmol/mol (Ullmann et al., 2013), ii) the calcium carbonate polymorph, iii) the species specific fractionation of the Sr/Ca ratio, iv) metabolic controls on this fractionation factor and v) water temperature. The Sr/Ca ratio in calcareous nannofossils is a relative proxy which has no quantitative calibration. The process underlying the positive relation between Sr/Ca and productivity stands on the observation that more Sr is incorporated in calcite with high calcification rates which positively correlates with high cell physiological rates. This proxy is also species-dependent or, at least, *group*-dependent (Stoll & Ziveri, 2004). The latter is discussed, the species-dependency may be related to different calcification physiologies (Payne et al., 2008; Suchéras-Marx et al., 2016b) or to different partitioning coefficients in relation to different ultrastructure organizations and more precisely between V- and R- crystals in coccoliths (Young et al., 1992) theoretically possible (Paquette & Reeder, 1995) but still not observed (Stoll & Ziveri, 2004).

Recently, analyses on the cultured murolith *Scyphosphaera apsteinii* showed Sr/Ca ~22 mmol/mol, an order of magnitude higher than the common ~1-4 mmol/mol measured in placoliths such as *Gephyrocapsa oceanica*, *Gephyrocapsa huxleyi*, *Calcidiscus leptoporus*, *Coccolithus pelagicus* or *Helicosphaera carteri* (Hermoso et al., 2017; Stoll et al., 2007). Hermoso et al. (2017) also highlight observations of high Sr/Ca in fossil muroliths *Pontosphaera* (Pliocene) and *Crepidolithus* (Lower Jurassic) but points out that *Scyphosphaera*, *Pontosphaera* and *Crepidolithus* have different crystal organizations and growth directions and thus crystal organization cannot explain murolith high Sr/Ca.

The present study aims to map Sr and Ca in *Crepidolithus crassus* and to compare the calculated Sr/Ca with the crystal growth directions in order to explain the murolith Sr anomaly. This study will discuss then the range of applicability and limitation of the Sr/Ca proxy in coccoliths.

2. Material and methods

1.1 Material

The coccolith analyzed in this study comes from sample CM35, a marlstone from the lower Bajocian (Middle Jurassic) of Cabo Mondego (Portugal; section in Suchéras-Marx et al., 2012). This section was selected because it is the Aalenian-Bajocian boundary GSSP (Pavia & Enay, 1997). A total of three coccoliths from three different species were studied, namely the murolith *Crepidolithus crassus* and two placoliths *Discorhabdus striatus* and *Watznaueria contracta*.

1.2 Sample preparation

The three coccoliths were picked using Suchéras-Marx et al. (2016a) protocol which consist in a hand-picking procedure. Rock powder is smeared on a cover slide in order isolate particles from each other. Coccoliths are then observed with an optical microscope Leica DM750P with a x200 magnification (x20 dry objective) under cross-polarized light. Coccoliths are identified with a x400 magnification (x40 dry objective) and a λ/4 gypsum filter may be used if further optical criteria of recognition are needed. Once picked, each coccolith is mounted on 500 nm-

thick silicon nitride (Si_3N_4) TEM windows (Silson Ltd. Southam, UK) using a drop of ethanol to detach the coccolith from the needle. No other chemical or physical treatment were made.

1.3 NanoXRF 17 keV mapping at ID22NI

The XRF analyses were performed at beamline ID22NI (currently ID16b) at the European Synchrotron Radiation Facility (ESRF), Grenoble, France. All three coccoliths were analyzed at an incident X-ray beam energy of 17 keV to ensure the measure of Sr (Kα = 14.165 keV). The beam spot was focused by an ESRF custom-made Kirkpatrick-Baez double multilayer mirror device to a 100 nm x 100 nm size. Each spot was analyzed for 2 s. The detectors were high-count rate twin SII™ vortex SDD (silicon drift diode) detectors, capable of counting up to 200 kcps with no saturation and no peak shift or FWHM broadening, when operated below 10% dead time. The sample is orthogonal to the incident beam and the detector is placed at a 15° angle relative to the sample surface. The three coccoliths were mapped. Each pixel corresponds to a spot of analysis and spots are adjacent provinding a full map of each coccolith. *Crepidolithus crassus* map is 136 x 120 pixels large, *D. striatus* is 60 x 34 pixels large and *W. contracta* map is 100 x 74 pixels large. The XRF analysis being penetrative, the element counting sum up the membrane, the coccolith and the air surrounding the coccolith. The contribution of the air is negligible, and the contribution of the membranes are estimated in Fig. 1 based on quantification in zones without the coccolith in the maps. All calculations were made using PyMCA 5.1.1. (Solé et al., 2007). This beam line set-up, analysis procedure and calculation fit are the same as in Suchéras-Marx et al. (2016b).

3. Results

1.4 XRF spectrum

The three spectra shown in Fig. 1 represent the mean spectrum for each coccolith. Because XRF analysis is penetrative, the spectra also record the membrane holding the coccolith and thus the spectrum of zones with only the membrane is also presented. The fit presented for each spectrum is the modeled reconstruction used for the calculation and the map reconstruction (cps and mmol/mol). In *D. striatus* and *W. contracta*, 14 elements are recorded namely: S, Cl, Ar, K, Ca, Mn, Fe, Cu, Zn, Br, Kr, Rb, Sr and Pb whereas in *C. crassus* only 12 are recorded (same elements except Kr and Rb) (Fig. 1). The rare gases Ar and Kr are present in the air in the experimental hutch. The contribution of the membrane is lower than 1% for Ca and Sr and thus is negligible for the Sr/Ca calculation. Nevertheless, membrane contribution was excluded in Table 1. Those results are similar to already published *W. britannica* and *D. striatus* (Suchéras-Marx et al., 2016b; Suchéras-Marx et al., 2021).

1.5 Element and ratio maps

For the three coccoliths, element maps of Ca, Mn and Sr are presented in Fig. 2 (cps) and the three maps together in color in Supplementary Figure 1. Direct comparison of Ca and Sr is possible in both placoliths whereas Mn is quite different although crystal organization is also observed in this element map. In *W. contracta*, the Ca maps are precise enough to recognize the shield crystal orientations, especially the outer radial growth from the tube ring. The tube structures are difficult to recognize but still, crystals can be seen in the rim around the central area. In the Sr map of the same species, the outer rim with radial crystals of the shields are easily observed too. A ring with slightly more Sr marks a boundary between the outer rim and the inner rim structures. These inner rim structures are composed of two concentric rings of crystal assemblages. The outermost one may correspond to the mid tube elements whereas the innermost one may correspond to the inner tube elements. The mid tube elements form a clear rim whereas one shield crystal assemblage is nicely depicted in the Mn map (Suchéras-Marx et al., 2016b). In *D. striatus*, the Sr seems less abundant in the tube units in comparison to the shield elements. For the same species, the Mn is scarce in the central area and the tube structures but more abundant in the shields.

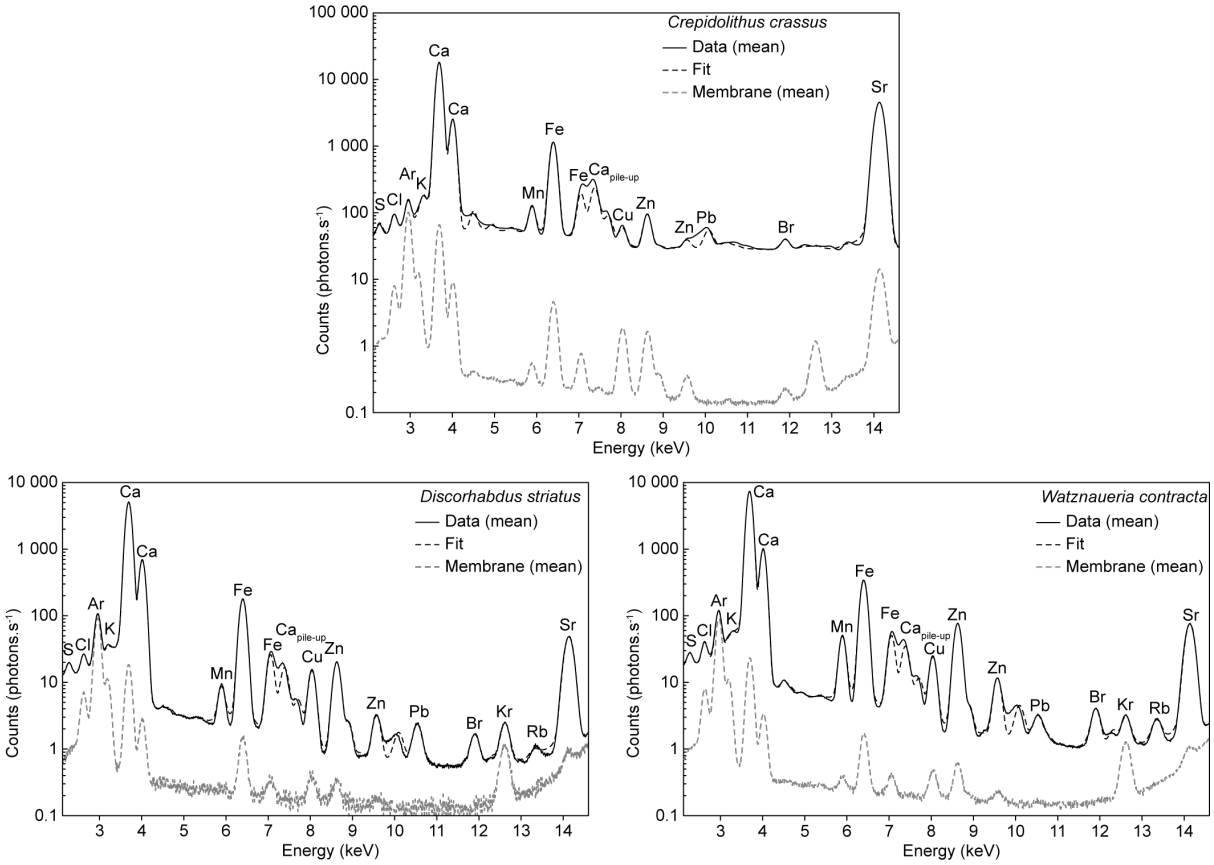

Figure 1. Mean XRF spectra of *C. crassus*, *D. striatus* and *W. contracta* coccoliths and associated membrane spectra. $Ca_{pile\text{-}up}$ correspond to the quantification of two Ca energy summed arriving at the same time in the captor. Ar is the same in coccolith and membrane because it corresponds to the air in the experimental hutch. In the three coccoliths, membrane contribution in Ca, Fe, Cu and Zn and in Sr in *C. crassus* is observed. However, it is always two order of magnitude below the concentration in the coccolith thus membrane contribution represents less than 1% in those elements.

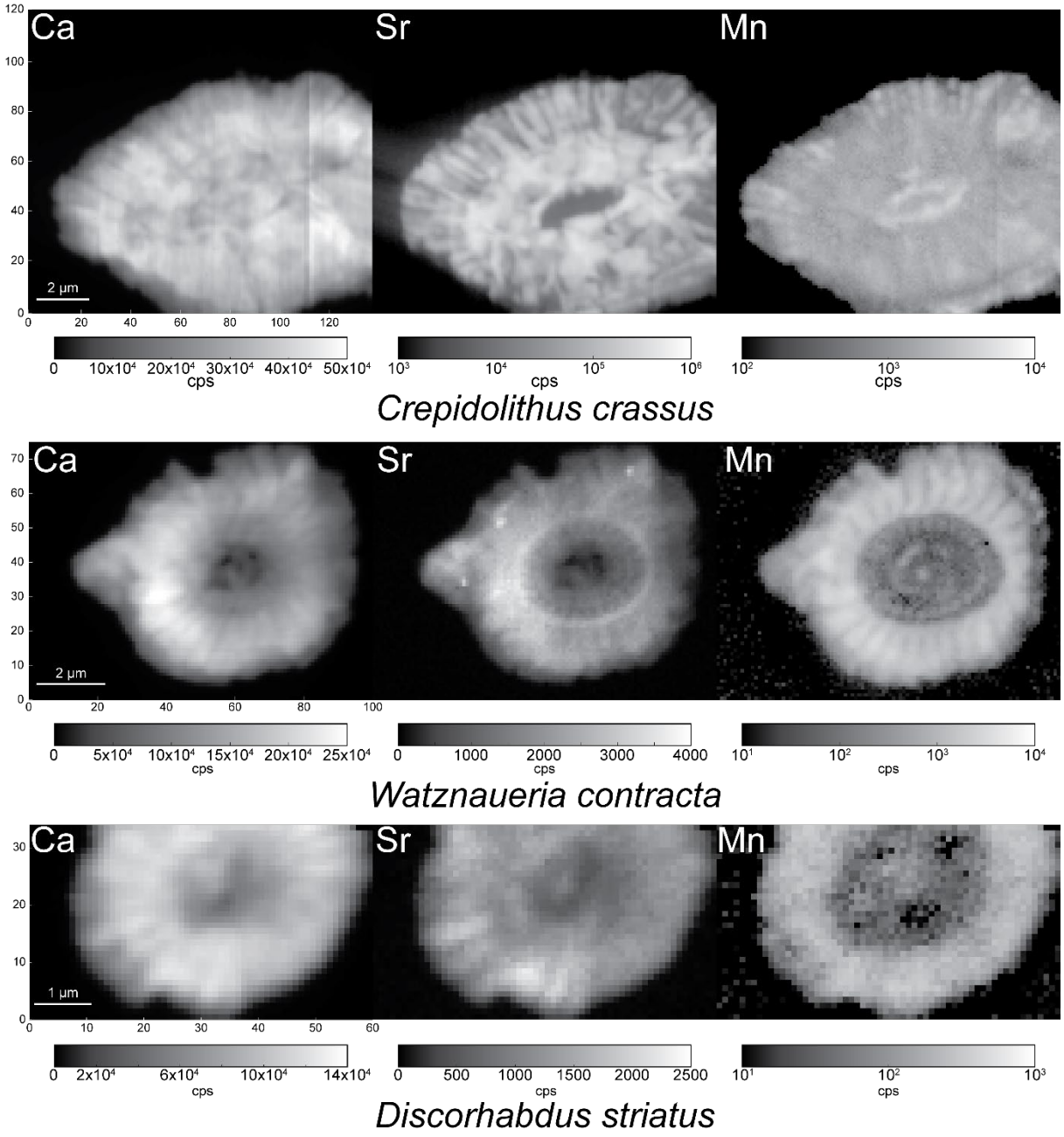

Figure 2. Ca, Mn and Sr maps (cps) of *C. crassus*, *D. striatus* and *W. contracta*.

Conversely to the placoliths, in *C. crassus*, the Ca and Sr maps are slightly different. In Sr maps, the central area is easily visible. Around the central area, an inner concentric rim of more abundant Sr is observed. A concentric outer rim up to the lateral border is observed with Sr concentrated in radial rays. In the Ca map, the outer rim is also observed in radial structures but the inner rim is distinguished from the outer only by a discontinuity. Finally, another discontinuity separates the central area from the inner rim.

	Mean whole coccolith		Selected zone	
element ratio (mmol/mol)	Mn/Ca	Sr/Ca	Mn/Ca	Sr/Ca
Crepidolithus crassus	0,75	9,82	0,92	17,70
Discorhabdus striatus	0,23	0,38	0,09	0,31
Watznaueria contracta	1,10	0,40	0,58	0,45

Table 1. Mn/Ca and Sr/Ca (mmol/mol) of whole coccoliths of *C. crassus*, *D. striatus* and *W. contracta* or a selected region (see Supplementary Figure 2), depleted in Mn and Fe.

For all species, the Sr/Ca maps have the same patterns as Sr and similarly, the Mn/Ca maps have the same patterns as Mn (Fig. 3). In *C. crassus* then, the Sr/Ca is higher in a ring around the central area and in radially oriented crystals in the outer ring. In the most concentrated area, the Sr/Ca ranges between 10 and 100 mmol/mol and tends to be two orders of magnitude higher than in *W. contracta* and *D. striatus*. Finally, the area with higher Sr/Ca is neither enriched nor depleted in Mn/Ca.

4. Discussion

A previous study already discussed the Sr/Ca signal in *Watznaueria* (Suchéras-Marx et al., 2016b), discussion that likely applies to *Discorhabdus*. The presence of other elements such as Cl, Fe or Zn won't be discussed here to focus on Sr/Ca. Nevertheless, according to Suchéras-Marx et al. (2016b) Cl and S may be incorporated in the coccolith during coccolithogenesis whereas K, Fe, Cu, Zn, Br and Rb are incorporated during diagenesis or are contaminant from clays. Recently, Bottini et al. (2020) studied coccolith from controlled cultures confirmed that V, Fe, Ni, Zn and Pb are not incorporated in coccolith calcite ; they also proposed that Cl is a contaminant from seawater not present in the coccolith crystal composition. Finally, the presence of Mn is related to overgrowth and diagenesis in both *Watznaueria* and *Discorhabdus* (Suchéras-Marx et al., 2016b; Suchéras-Marx et al., 2021). The three coccoliths are coming from the same sample and were analyzed with the same set-up, thus the very high Sr/Ca in *C. crassus* compared to *W. contracta* and *D. striatus* is not related to analytical biases and to seawater Sr/Ca. Moreover, the Sr-rich rim in *C. crassus* is not enriched in Mn and thus the high Sr/Ca in *C. crassus* is not related to diagenesis. Finally, the calculated Sr/Ca for the lower Bajocian seawater ranges between 4 mmol/mol and 6.8 mmol/mol (Ullmann et al., 2013) below most modern oceanic environments (Lebrato et al., 2020) and thus cannot explain the high Sr/Ca in *C. crassus*. This result is coherent with a previous study observing that diagenesis tends to lower Sr/Ca in calcareous nannofossils (Dedert et al., 2014) as Sr concentrations are relatively high in seawater and are low in diagenetic fluids (Veizer, 1974; James & Jones, 2016).

The Sr anomaly in *C. crassus* is then related to either i) an ion pump concentrating the Sr^{2+} inside the cell to higher concentrations than other species; ii) the use of a polysaccharide that tends to increase Sr/Ca in comparison to other species or iii) the crystal organization and growth directions which are controlled by the cell but the high concentration in Sr would then be a by-product of the coccolith construction. Obviously, *C. crassus* being a fossil occurring only during the Jurassic, the cell biology of the species cannot be explored. Nevertheless, this species is a large murolith like the extant *Pontosphaera discopora* and has a similar shape to the extant *Scyphosphaera apsteinii*'s lopadolith, both having also higher Sr/Ca than the common placoliths' signature of 1-4 mmol/mol (Hermoso et al., 2017).

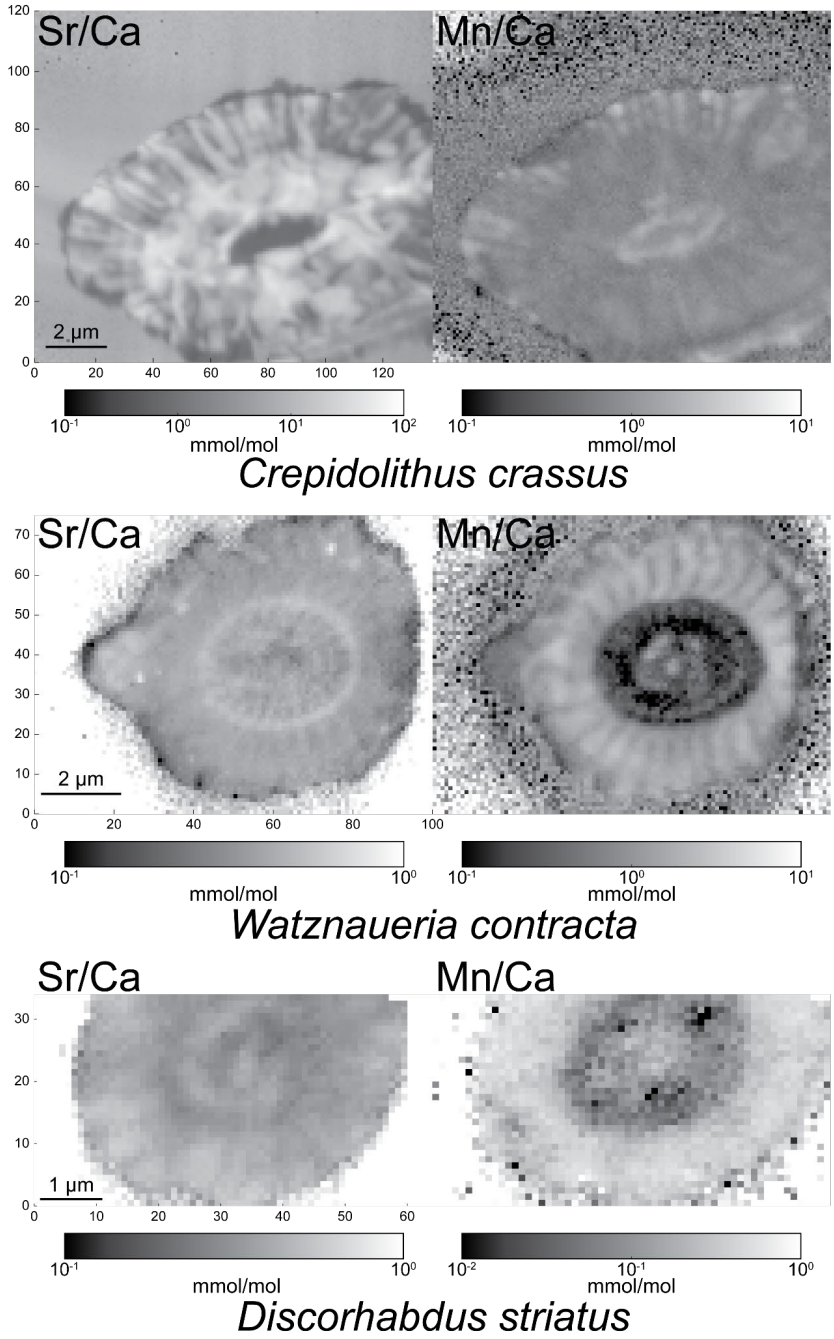

Figure 3. Mn/Ca and Sr/Ca (mmol/mol) maps of *C. crassus*, *D. striatus* and *W. contracta*.

The first two hypotheses (*i.e.* Sr^{2+} ion pump or special polysaccharide) could be that high Sr/Ca is inherited in descendant species from *C. crassus*. Both *Pontosphaera* and *Scyphosphaera* are very closely related in the coccolithophore phylogeny (family Pontosphaeraceae; de Vargas et al., 2007). *Crepidolithus* is within the family Chiastozygaceae (Bown & Young, 1998), whose position is unknown, but could be the ancestor of the family Zygodiscaceae and its descendants, the families Pontosphaeraceae and Helicosphaeraceae (Bown & Young, 1998). Thus, the high Sr/Ca in both *Pontosphaera* and *Scyphosphaera* could be an ancestral character inherited from *Crepidolithus*. This hypothesis may be challenged by *Helicosphaera carterii* which has a Sr/Ca ratio around 2-3 mmol/mol (Stoll & Ziveri, 2004) and is from the family Helicosphaeraceae, the sister group of the family Pontosphaeraceae (Bown & Young, 1998). The low Sr/Ca in *H. carterii* could then be a derived character in the phylogeny, arguing for a phyletic heritage of *Pontosphaera* and *Scyphosphaera* from *Crepidolithus* or this character is ancestral in the family Helicosphaeraceae and the Sr/Ca is not linked to the phylogeny. The current knowledge on coccolithophore phylogeny and Sr/Ca cannot exclude one or the other solutions, hence a possible ion pump or

polysaccharide could have favored the high Sr/Ca in *C. crassus*. Recently, Meyer et al. (2020) observed that Sr^{2+} and Ca^{2+} fluxes in the coccolith vesicle for coccolithogenesis does not solely govern Sr incorporation in the coccolith speculating than that possible species-specific polysaccharides dedicated to a peculiar coccolith morphology may act in the high Sr/Ca observed in *Scyphosphaera*.

The last hypothesis relies on the fact that *C. crassus*, *P. discopora* and *S. apsteinii* have the same shape (*i.e.* murolith and lopadolith) and are very large coccoliths, thus the shape and size may influence the Sr incorporation in coccolith calcite. The large size of those coccoliths cannot be the main reason of high Sr/Ca because *Coccolithus braarudii*, a very large placolith, has Sr/Ca equivalent to very small placoliths (*i.e. G. huxleyi*; Müller et al., 2011). The basic crystal organization of heterococcoliths is explained by the V/R model which describes the crystal growth in the *c-axis* whether radially (*i.e.* R-unit) or vertically (*i.e.* V-unit) from a primary ring of crystals called protococcolith (Young et al., 1992). In *C. crassus*, the V-units are more developed than the R-units (Fig. 4), whereas in *P. discopora* and *S. apsteinii* V-units represent only the narrow outer part of the rim wall (Young & Bown, 1997; Fig. 4). According to Hermoso et al. (2017), the growth of calcite in the same direction as the *c-axis* should favor Sr^{2+} incorporation but the R-units in *P. discopora* and *S. apsteinii* actually grow longer in the vertical axis hence grow orthogonally to the *c-axis*. In the case of *C. crassus*, the Sr/Ca is higher around the central area which corresponds to the proximal cycle formed by R-units. Counter-intuitively for these three species with thick vertical walls, the Sr is concentrated in the R-units. Surprisingly, *C. crassus* R-units are, like *P. discopora* and *S. apsteinii*, more elongated vertically than radially, thus the growth seems orthogonal to the *c-axis* (Fig. 4). Then, either the orthogonal to *c-axis* growth actually favors Sr^{2+} contradicting Hermoso et al. (2017) or the biomolecule acting in this growth direction has more affinities with Sr^{2+} than the other polysaccharides.

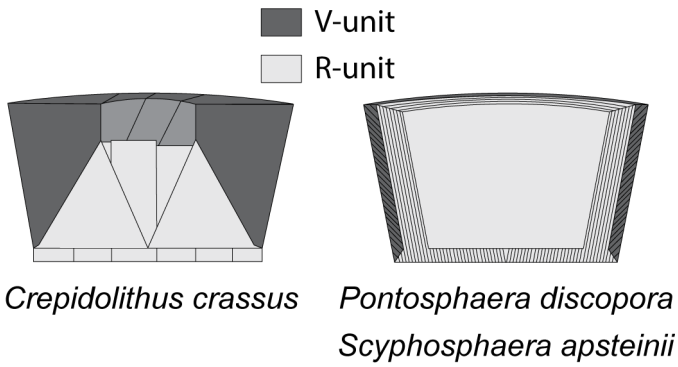

Figure 4. Crystal assembly of *Crepidolithus, Pontosphaera* and *Scyphosphaera*. R-units (light grey) and V-units (dark grey), derived from Bown & Young, 1998.

5. Conclusion

Despite the very high and continuous fossil record of coccoliths since the Late Triassic, the use of geochemical analyses on these calcite platelets for paleoenvironmental reconstructions remain rare. So far, coccolith Sr/Ca is the only coccolith-based geochemical proxy commonly used in paleoceanography. Yet, there are many unknown features about this productivity proxy such as the very high Sr/Ca (*i.e.* above ~10 mmol/mol) in some species namely *S. apsteinii*, *P. discopora* and *C. crassus*. In this study, we compared Sr/Ca of *C. crassus* to contemporaneous placoliths using synchrotron-based nanoXRF and observed that:

C. crassus has higher Sr/Ca than contemporaneous placoliths;

C. crassus Sr/Ca map is different than the Mn/Ca map

Sr/Ca in *C. crassus* is higher in the proximal cycle than in the distal cycle

Hence, high *C. crassus* Sr/Ca, is not linked to diagenetic overgrowth or seawater Sr/Ca but may be related to vertical elongation of R-units and/or affinity to Sr^{2+} of the polysaccharide responsible for the growth of those peculiar R-units. The use of murolith's Sr/Ca in the future may be interesting due to their high values, easier to measure and to the large size of these coccoliths, easier to separate from the bulk placoliths. Nevertheless, in order to apply the Sr/Ca productivity proxy to muroliths in the future, new culture studies should test the relation between Sr incorporation and growth rate. The study of *Pontosphaera* or *Scyphosphaera* with 3D nanoXRF will

directly link Sr/Ca relative concentration with coccolith crystal organization and thus would clearly improve the understanding of the Sr anomaly in those coccoliths.

6. Author contributions

BSM, FG and ID designed the study with later contribution from AS. BSM, FG, ID, AS and RT did the analyses. BSM performed the data treatment with help from AS. BSM wrote the manuscript with comments from all contributors.

7. Data accessibility

Data presented in this study are freely accessible on PANGAEA database (https://doi.org/10.1594/PANGAEA.913826). Related data produced with similar material and during the same ESRF experiment (project EC811) are also accessible on PANGAEA with https://doi.pangaea.de/10.1594/PANGAEA.913813 published in Suchéras-Marx et al. (2016), https://doi.pangaea.de/10.1594/PANGAEA.913811 in Suchéras-Marx et al. (under revision (preprint version available)) and unpublished data (https://doi.pangaea.de/10.1594/PANGAEA.914203).

8. Acknowledgments

We acknowledge the ESRF for providing access to synchrotron radiation on the ID22NI beamline through proposal EC811. We deeply thank the recommender Antonino Briguglio and the reviewer Kenneth De Baets as well as the anonymous reviewer for suggestions that clearly improved the manuscript. BSM is particularly proud to be recommended in PCIPaleo and hope this editorial model will develop in the future. This study is a contribution to the Cerege's team 'Climat'.

9. Conflict of interest disclosure

The authors declare that they have no financial conflict of interest with the content of this article. None of the authors is a PCI Paleo recommender.

10. References

Bottini C, Dapiaggi M, Erba E, Faucher G, Rotiroti N (2020) High resolution spatial analyses of trace elements in coccoliths reveal new insights into element incorporation in coccolithophore calcite. *Scientific Reports*, **10**, 9825. https://doi.org/10.1038/s41598-020-66503-x

Bown PR, Young JR (1998) Introduction in: Bown PR (Ed.), Calcareous nannofossil biostratigraphy. *British Micropaleontological Society Publication Series*. Chapman and Hall (Kluwer Academic Publishers), Dondrecht, pp. 1–15.

Dedert M, Stoll HM, Kars S, Young JR, Shimizu N, Kroon D, Lourens LJ, Ziveri P (2014) Temporally variable diagenetic overgrowth on deep-sea nannofossil carbonates across Palaeogene hyperthermals and implications for isotopic analyses. *Marine Micropaleontology*, **107**, 18–31. https://doi.org/10.1016/j.marmicro.2013.12.004

Elderfield H, Ganssen G (2000). Past temperature and $\delta^{18}O$ of surface ocean waters inferred from foraminiferal Mg/Ca ratios. *Nature*, **405**, 442–445. https://doi.org/10.1038/35013033

Hermoso M, Lefeuvre B, Minoletti F, de Rafélis M (2017) Extreme strontium concentrations reveal specific biomineralization pathways in certain coccolithophores with implications for the Sr/Ca paleoproductivity proxy. *PLoS ONE*, **12**, e0185655. https://doi.org/10.1371/journal.pone.0185655

James NP, Jones B (2015) Origin of carbonate sedimentary rocks. *Wiley-Blackwell*, 464 p.

Lebrato M, Garbe-Schönberg D, Müller MN, Blanco-Ameijeiras S, Feely RA, Lorenzoni L, Molinero J-C, Bremer K, Jones DOB, Iglesias-Rodriguez D, Greeley D, Lamare MD, Paulmier A, Graco M, Cartes J, Barcelos e Ramos J, de Lara A, Sanchez-Leal R, Jimenez P, Paparazzo FE, Hartman SE, Westernströer U, Küter M, Benavides R, da Silva AF, Bell S, Payne C, Olafsdottir S, Robinson K, Jantunen LM, Korablev A, Webster RJ, Jones EM, Gilg O, Bailly du

Bois P, Beldowski J, Ashjian C, Yahia ND, Twining B, Chen X-G, Tseng L-C, Hwang J-S, Dahms H-U, Oschlies A (2020) Global variability in seawater Mg:Ca and Sr:Ca ratios in the modern ocean. *Proceedings of the National Academy of Sciences*, **117**, 22281–22292. https://doi.org/10.1073/pnas.1918943117

Meyer EM, Langer G, Brownlee C, Wheeler GL, Taylor AR (2020) Sr in coccoliths of *Scyphosphaera apsteinii*: Partitioning behavior and role in coccolith morphogenesis. *Geochimica et Cosmochimica Acta*, **285**, 41–54. https://doi.org/https://doi.org/10.1016/j.gca.2020.06.023

Minoletti F, Hermoso M, Gressier V (2009) Separation of sedimentary micron-sized particles for palaeoceanography and calcareous nannoplankton biogeochemistry. *Nature Protocols*, **4**, 14–24. https://doi.org/10.1038/nprot.2008.200

Müller MN, Kisakürek B, Buhl D, Gutperlet R, Kolevica A, Riebesell U, Stoll H, Eisenhauer A (2011) Response of the coccolithophores *Emiliania huxleyi* and *Coccolithus braarudii* to changing seawater Mg^{2+} and Ca^{2+} concentrations: Mg/Ca, Sr/Ca ratios and $\delta^{44/40}Ca$, $\delta^{26/24}Mg$ of coccolith calcite. *Geochimica et Cosmochimica Acta*, **75**, 2088–2102. https://doi.org/10.1016/j.gca.2011.01.035

Paquette J, Reeder RJ (1995) Relationship between surface structure, growth mechanism, and trace element incorporation in calcite. *Geochimica et Cosmochimica Acta*, **59**, 735–749. https://doi.org/10.1016/0016-7037(95)00004-J

Pavia G, Enay R (1997) Definition of the Aalenian-Bajocian Stage boundary. *Episodes*, **20**, 16–22. https://doi.org/10.18814/epiiugs/1997/v20i1/004

Payne VE, Rickaby REM, Benning LG, Shaw S (2008) Calcite crystal growth orientation: implications for trace metal uptake into coccoliths. *Mineralogical Magazine*, **72**, 269–272. https://doi.org/10.1180/minmag.2008.072.1.269

Raitzsch M, Kuhnert H, Hathorne EC, Groeneveld J, Bickert T (2011) U/Ca in benthic foraminifers: A proxy for the deep-sea carbonate saturation. *Geochemistry, Geophysics, Geosystems*, **12**, Q06019. https://doi.org/10.1029/2010gc003344

Rickaby REM, Elderfield H (1999) Planktonic foraminiferal Cd/Ca: Paleonutrients or Paleotemperature? *Paleoceanography*, **14**, 293–303. https://doi.org/10.1029/1999PA900007

Solé VA, Papillon E, Cotte M, Walter P, Susini J (2007) A multiplatform code for the analysis of energy-dispersive X-ray fluorescence spectra. *Spectrochimica Acta Part B: Atomic Spectroscopy*, **62**, 63–68. https://doi.org/10.1016/j.sab.2006.12.002

Stoll HM, Schrag DP (2000) Coccolith Sr/Ca as a new indicator of coccolithophorid calcification and growth rate. *Geochemistry, Geophysics, Geosystems*, **1**, 1006. https://doi.org/10.1029/1999GC000015

Stoll HM, Shimizu N (2009) Micropicking of nannofossils in preparation for analysis by secondary ion mass spectrometry. *Nature Protocols*, **4**, 1038–1043. https://doi.org/10.1038/nprot.2009.83

Stoll HM, Ziveri P (2002) Separation of monospecific and restricted coccolith assemblages from sediments using differential settling velocity. *Marine Micropaleontology*, **46**, 209–221. https://doi.org/10.1016/S0377-8398(02)00040-3

Stoll HM, Ziveri P (2004) Coccolithophorid-based geochemical paleoproxies, in: Thierstein HR, Young JR (Eds.), *Coccolithophores: From molecular processes to global impact*. Springer, Verlag, pp. 529–562. https://doi.org/10.1007/978-3-662-06278-4_20

Stoll HM, Shimizu N, Arevalos A, Matell N, Banasiak A, Zeren S (2007) Insights on coccolith chemistry from a new ion probe method for analysis of individually picked coccoliths. *Geochemistry, Geophysics, Geosystems*, **8**, Q06020. https://doi.org/10.1029/2006GC001546

Suchéras-Marx B, Guihou A, Giraud F, Lécuyer C, Allemand P, Pittet B, Mattioli E (2012) Impact of the Middle Jurassic diversification of *Watznaueria* (coccolith-bearing algae) on the carbon cycle and $\delta^{13}C$ of bulk marine carbonates. *Global and Planetary Change*, **86-87**, 92–100. https://doi.org/10.1016/j.gloplacha.2012.02.007

Suchéras-Marx B, Giraud F, Lena A, Simionovici A (2016a) Picking nannofossils: How and why. *Journal of Micropalaeontology*, **36**, 219–221. https://doi.org/10.1144/10.1144jmpaleo2016-013

Suchéras-Marx B, Giraud F, Simionovici A, Daniel I, Tucoulou R (2016b) Perspectives on heterococcolith geochemical proxies based on high-resolution X-ray fluorescence mapping. *Geobiology*, **14**, 390–403. https://doi.org/10.1111/gbi.12177

Suchéras-Marx B, Giraud F, Daniel I, Rivard C, Aubry M-P, Baumann K-H, Beaufort L, Tucoulou R, Simionovici A (2021) Origin of manganese in coccolith calcite based on synchrotron nanoXRF and XANES. *Marine Micropaleontology*, **163**, 101961. https://doi.org/https://doi.org/10.1016/j.marmicro.2021.101961

Ullmann CV, Hesselbo SP, Korte C (2013) Tectonic forcing of Early to Middle Jurassic seawater Sr/Ca. *Geology*, **41**, 1211–1214. https://doi.org/10.1130/G34817.1

Vargas C de, Aubry M-P, Probert I, Young JR (2007) Origin and evolution of coccolithophores: From coastal hunters to oceanic farmers, in: Falkowski PG, Knoll A (Eds.), *Evolution of primary producers in the sea*. Academic Press, pp. 251–286. https://doi.org/10.1016/B978-012370518-1/50013-8

Veizer J (1974) Chemical diagenesis of belemnite shells and possible consequences for paleotemperature determinations. *Neues Jahrbuch für Geologie und Paläontologie, Abhandlungen*, **147**, 91–111.

Young JR, Bown PR (1997) Higher classification of calcareous nannofossils. *Journal of Nannoplankton Research*, **19**, 15–20.

Young JR, Didymus JM, Bown PR, Mann S (1992) Crystal assembly and phylogenetic evolution in heterococcoliths. *Nature*, **356**, 516–518. https://doi.org/10.1038/356516a0

Yu J, Elderfield H, Hönish B (2007) B/Ca in planktonic foraminifera as a proxy for surface seawater pH. *Paleoceanography*, **22**, 2202. https://doi.org/10.1029/2006PA001347

11. Supplementary figures

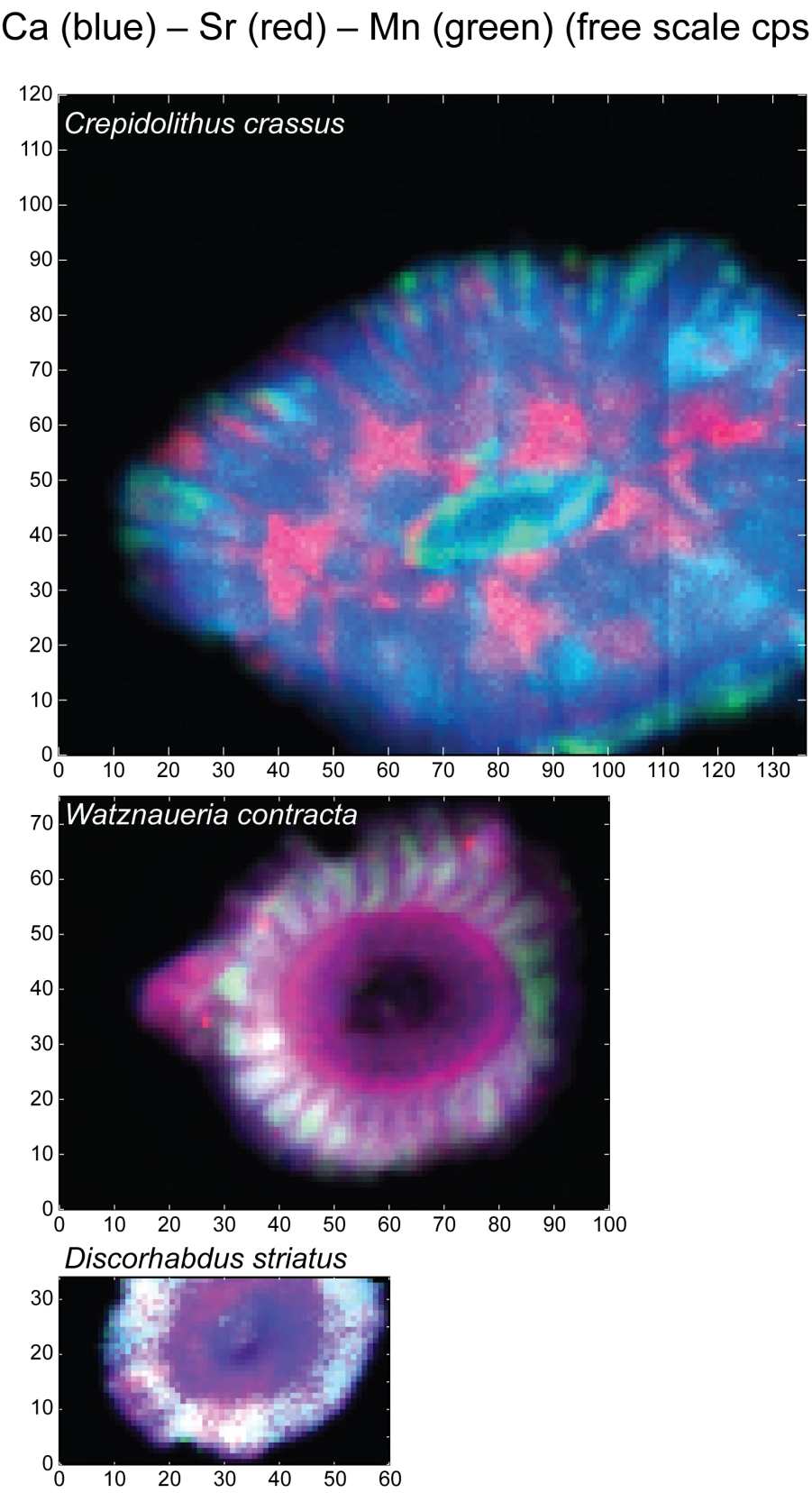

Supplementary Figure 1. Ca (blue), Sr (red) and Mn (green) maps (free scale cps) of *C. crassus*, *W. contracta* and *D. striatus*.

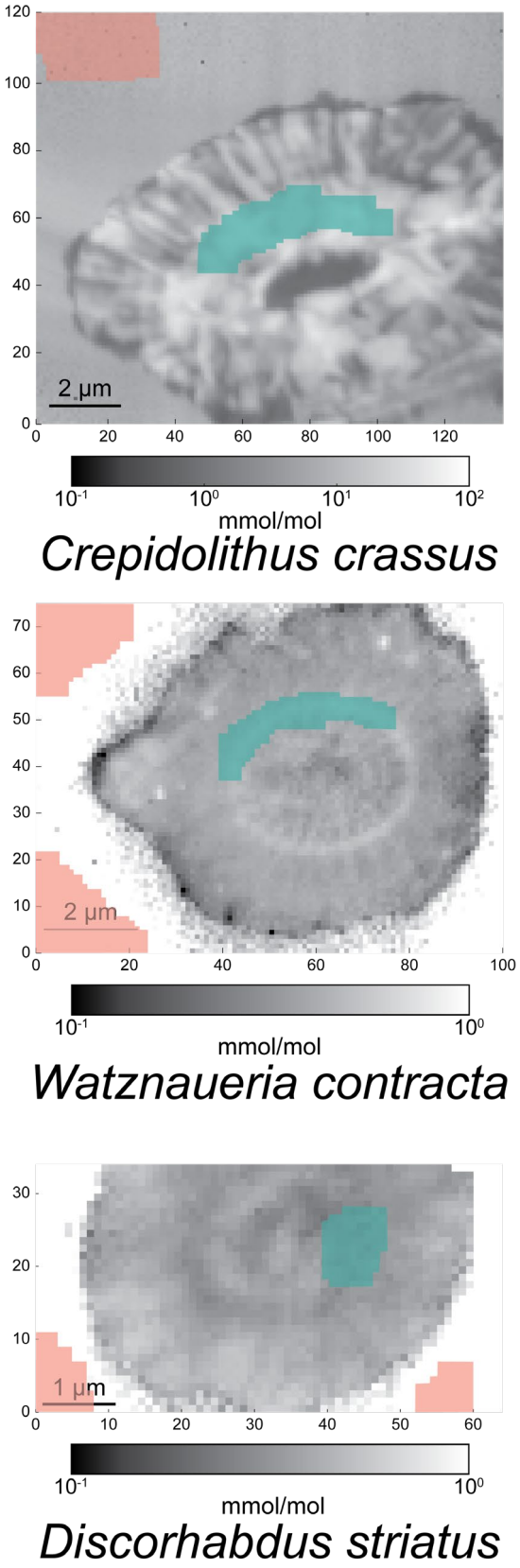

Supplementary Figure 2. Selected zone (green) and background (red) used for calculations in Table 1 over Sr/Ca (mmol/mol) maps for *C. crassus*, *W. contracta* and *D. striatus*.